


# Comparing position and orientation accuracy of different electromagnetic sensors for tracking during interventions

Jasper Nijkamp<sup>1</sup>  · Bram Schermers<sup>1</sup> · Sander Schmitz<sup>1</sup> · Sofieke de Jonge<sup>1</sup> · Koert Kuhlmann<sup>1</sup> · Ferdinand van der Heijden<sup>2</sup> · Jan-Jakob Sonke<sup>3</sup> · Theo Ruers<sup>1</sup>

Received: 3 August 2015 / Accepted: 30 December 2015 / Published online: 25 January 2016  
© CARS 2016

## Abstract

**Purpose** To compare the position and orientation accuracy between using one 6-degree of freedom (DOF) electromagnetic (EM) sensor, or the position information of three 5DOF sensors within the scope of tumor tracking.

**Methods** The position accuracy of Northern Digital Inc Aurora 5DOF and 6DOF sensors was determined for a tabletop field generator (TTFG) up to a distance of 52 cm. For each sensor 716 positions were measured for 10 s at 15 Hz. Orientation accuracy was determined for each of the orthogonal axis at the TTFG distances of 17, 27, 37 and 47 cm. For the 6DOF sensors, orientation was determined for sensors in-line with the orientation axis, and perpendicular. 5DOF orientation accuracy was determined for a theoretical 4 cm tumor. An optical tracking system was used as reference.

**Results** Position RMSE and jitter were comparable between the sensors and increasing with distance. Jitter was within 0.1 cm SD within 45 cm distance to the TTFG. Position RMSE was approximately 0.1 cm up to 32 cm distance, increasing to 0.4 cm at 52 cm distance. Orientation accuracy of the 6DOF sensor was within 1°, except when the sensor was in-line with the rotation axis perpendicular to the TTFG plane (4° errors at 47 cm). Orientation accuracy using 5DOF positions was within 1° up to 37 cm and 2° at 47 cm.

**Conclusions** The position and orientation accuracy of a 6DOF sensor was comparable with a sensor configuration consisting of three 5DOF sensors. To achieve tracking accuracy within 1 mm and 1°, the distance to the TTFG should be limited to approximately 30 cm.

**Keywords** Tumor tracking · Electromagnetic tracking · Position accuracy · Orientation accuracy

## Introduction

Surgical navigation has advanced to daily clinical routine in a variety of fields, such as neuro- and facial surgery, cochlear implantation and orthopedic oncology [1–5]. These fields have in common that the target area is relatively rigid due to surrounding bony structures. Most navigation systems assume no anatomical changes between the pre-operative images and the actual surgical setting.

During abdominal surgery, the anatomy of the patient is changing constantly due to breathing, peristalsis, and the surgery itself. As a consequence, there is a discrepancy between the preoperative imaging information and the actual anatomy, limiting the accuracy of navigation. For organs of which a large part of the surface can be visualized on laparoscopic images, e.g. liver, a manual surface registration can be used to utilize navigation during surgery [6, 7]. The changes in the anatomical position of a target organ can also be monitored automatically using optical tracking systems (OTS) or electromagnetic tracking systems (EMTS). OTS are known for their sub-millimeter accuracy, but are dependent on a direct line-of-sight to the target volume [8]. EMTS can provide tracking data independent of a line-of-sight, but are less accurate and can be influenced by surrounding materials and equipment. If a direct line of sight can be achieved, OTS

✉ Jasper Nijkamp  
j.nijkamp@nki.nl

<sup>1</sup> Department of Surgery, The Netherlands Cancer Institute – Antoni van Leeuwenhoek Hospital, Plesmanlaan 121, 1066 CX Amsterdam, The Netherlands

<sup>2</sup> Department of Robotics and Mechatronics, MIRA Institute for Biomedical Technology and Technical Medicine, University of Twente, Enschede, The Netherlands

<sup>3</sup> Department of Radiation Oncology, Netherlands Cancer Institute – Antoni van Leeuwenhoek Hospital, Amsterdam, The Netherlands

is preferred, such as in maxillofacial, neuro and orthopedic surgery. In abdominal applications, it is hard to see the targets, and EMTS seems more preferred.

NDI (Northern Digital Inc, Waterloo, Canada) is the current market leader in EMTS hardware, with the NDI Aurora and Microbird Ascension system in their portfolio. For the Aurora system, wired 5 degrees of freedom (DOF) and 6DOF sensors are available with a diameter of  $\leq 1$  mm and a length of about 10 mm, as well as tracked 5DOF needles of 18 or 21 Gauge. One or more sensors or needles in or around the abdominal tumor can be used to take anatomical changes into account. For example, Zhang et al. [9] proposed a setup for percutaneous liver interventions in which three tracked NDI needles were implanted near the target area to track breathing motion.

In locally advanced rectal cancer, incomplete surgery is performed in 20–30 % of patients [10, 11]. In these patients, the use of navigation might improve clinical outcome. For navigation during rectal cancer surgery, the use of a hybrid optical and electromagnetic tracking system was proposed by Wagner et al. [12]. In their experimental setup, one single 5DOF tracking sensor was placed in the rectum wall of a realistic phantom for assessment of displacements. Several models were used to translate the sensor displacements to rectum wall deformations. The evaluated models included simple rigid translation correction, up to complex organ modeling using combinations of independent elements. With rigid translations they were able to reduce the mean target registration error (TRE) from 32.8 mm down to 6.8 mm. Despite the major improvement using the position of an implanted sensor, the resulting accuracy was still insufficient for clinical practice. The most complex model (33 parameters) resulted in a mean TRE of 2.9. However, it is questionable if such a complex model can also be defined in real patient anatomy including a rectum tumor which might alter the mechanical properties.

To further improve tracking accuracy, the standard bedside Aurora electromagnetic field generator can be replaced by the more accurate tabletop field generator (TTFG) [13]. Also, position information could be improved by using more than one EM sensor. Finally, besides position information, the orientation of the tumor could be taken into account. Orientation information can be determined using one single 6DOF sensor, two combined 5DOF sensors, preferably positioned in a  $90^\circ$  angle, or three or more implanted sensors of which the position information is used to determine the orientation. Single 6DOF sensors generally consist of two combined 5DOF sensor coils, of which the data are combined to 6DOF within the EMTS system. The angle and distance between the 2 sensors is important for the orientation accuracy. Combining 2 separate 5DOF sensors enables freedom to change the distance and angle between the sensors.

For accuracy measurements, the use of a precisely machined base plate at different positions and distances to the TTFG was proposed by Hummel et al. and further improved by Maier-Hein et al. [13, 21]. In their work the accuracy of EMT is derived from comparing measured distances between sensor positions to known distances. This setup allows for accurate relative error measurements in the plane of base plate, but has limited value in providing absolute 3D local errors throughout the EM field. There is limited literature comparing the accuracy of 5DOF and 6DOF sensors in terms of position and orientation accuracy and jitter. The position accuracy of the 6DOF sensor seems to be equal [14] or slightly better than the 5DOF sensors [15]. The actual orientation accuracy with the different setups is unknown and is dependent on the sensor distances in the multi-sensor approaches.

Electromagnetic tracking systems has a large potential for tracking organs, tumors or equipment during complex interventions without the need for a line of sight. The purpose of the current study was to evaluate position and orientation accuracy using either one 6DOF sensor or the position information of multiple 5DOF sensors. Position accuracy of the sensors was determined throughout the entire EM field on a grid with 5 cm spacing and the orientation accuracy at several distances to the TTFG. In order to evaluate absolute errors, we used an OTS as reference. This setup allows for assessment of 3D errors throughout the measurement volume.

## Materials and methods

### Hardware

The EMTS was an NDI Aurora V2 TTFG with an oval work field of  $42 \times 60 \times 60$  cm in  $x$ -,  $y$ -, and  $z$ -direction (Fig. 1). No data can be measured in the first 12 cm above the TTFG. All position and orientation measurements were taken using an OTS as reference. The OTS was a NDI Polaris Spectra Hybrid system in which only passive reflective markers were used. The accuracy of this system is known to be  $< 0.025$  cm root-mean-square error (RMSE) [8]. In total, three different NDI sensors were evaluated. For 5DOF, we used the shielded and isolated  $0.9 \times 12$  mm sensors ( $5D_{\text{shielded}}$ ). For 6DOF, the micro  $0.8 \times 9$  mm sensors ( $6D_{\text{rod}}$ ) and the reference disks ( $6D_{\text{disk}}$ ) were evaluated. The  $6D_{\text{rod}}$  sensor consists of two combined 5DOF sensors, but the actual configuration of the sensor is unknown to us. The  $6D_{\text{disk}}$  contains two 5DOF sensors positioned in an angle of approximately  $90^\circ$  and was only used for orientation accuracy measurements to illustrate the accuracy with an optimized angle between the two 5DOF sensors.

To measure the entire EM field, an in-house built measurement setup was used. The TTFG was tightly encased by

a polycarbonate frame, on which an optical 4-marker rigid body tool was attached as a reference tool (Fig. 1). For evaluation of the position accuracy, four sensors were mounted on a sensor plate with 5 cm in between them. The sensor plate was positioned parallel to the TTFG (in the  $x - y$ -plane) starting at 12 cm from the TTFG ( $z$ -axis). The distance to the TTFG was configurable using stackable boxes. On the sen-

sor plate, three reflective spheres were mounted for optical tracking.

For evaluation of the orientation accuracy, a separate sensor construction was designed consisting of two plates coupled to each other with a revolute joint. With this construction the rotational axis of the joint could be aligned with each of the three orthogonal axes of the TTFG. The position and orientation of one of the sensor plates was determined by the OTS using three optical markers that were attached to this plate. For evaluation of the sensor orientation of the  $6D_{rod}$  with respect to the rotation axis, the rod-like sensor could be positioned in line or perpendicular to the rotational axis (Fig. 2). For evaluation of orientation accuracy using position information of multiple  $5D_{shielded}$  sensors, three sensors could be mounted on the sensor plate in a plane perpendicular to the rotation axis, with the sensors at distances of 28.2, 31.6, and 36.4 mm. This setup mimics implantation of three sensors within a tumor with a diameter of 40 mm. The rotational sensor plate could be placed anywhere within the EM field.

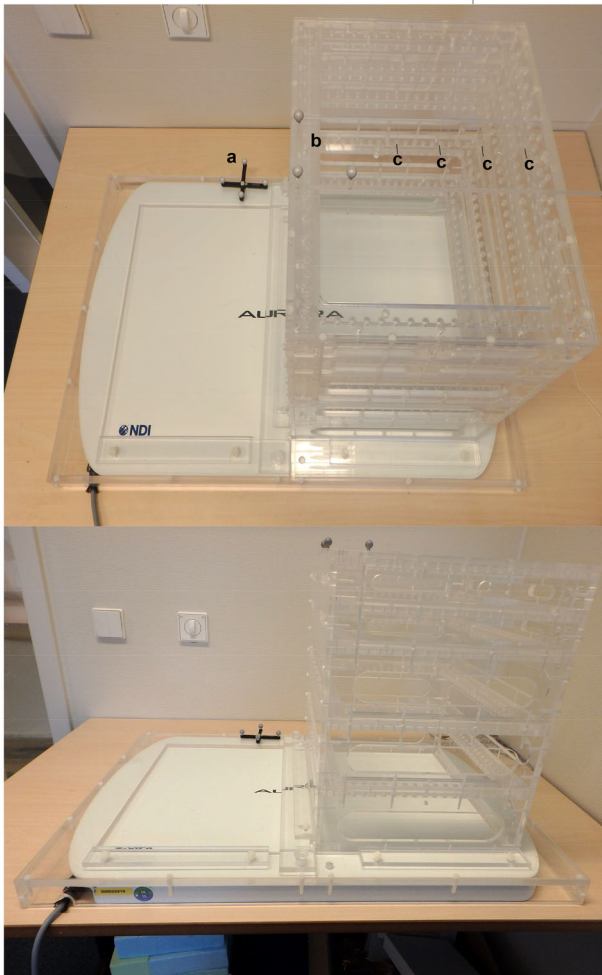
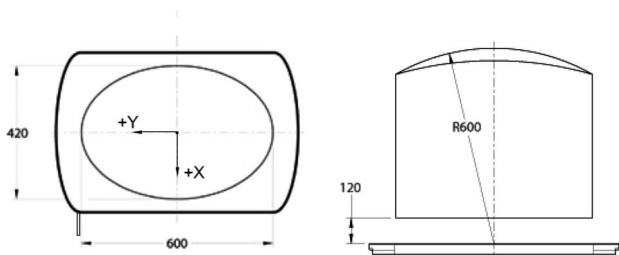


**Fig. 1** Top schematic overview of the work field and coordinate system of the TTFG (field dimensions in mm, [www.ndigital.com](http://www.ndigital.com)). Middle photo of the position measurement setup with a four marker optical reference tool on the TTFG case (a), an optical three marker rigid body tool on the sensor plate (b) in combination with four  $5D_{shielded}$  EM tools (c). Bottom side view of the measurement setup at 42 cm distance to the TTFG

## Software

In-house developed software was used for the data acquisition, using Embarcadero Delphi XE2 for the user interface, and a library of C++ modules for image and data processing. All tracking information was communicated using OpenIGTLink TRANSFORM messages. For readout of the NDI hardware the PlusServer from the Plus Toolkit (<https://www.assembla.com/spaces/plus/wiki>) was used [16]. Our in-house developed software used the OpenIGTLink.dll from IGSTK ([www.igstk.org](http://www.igstk.org)) to receive and translate the OpenIGTLink messages. Within PlusServer the data for the OTS and EMTS were combined into one data stream. Acquisition delays between the OTS and EMTS were also corrected within PlusServer. For averaging of orientations, the transformation matrices were converted to quaternions. The EMTS and OTS were connected to the same PC (Quad-core 3.2 GHz Intel Xeon E3-1230, with 16GB memory) using USB 2.0 connections.

## Calibration procedure

In order to use the OTS as a reference for the EMTS position measurements, a calibration procedure was performed for each set of sensors. Calibration was used to register both coordinate systems and to find the relation between the optical markers on the sensor plate and each of the EM sensors. In general, each measurement consisted of:

1. the pose (position and orientation) of the four EM sensors ( $S_x$ ,  $x = 1, \dots, 4$ ) expressed in the EM coordinate

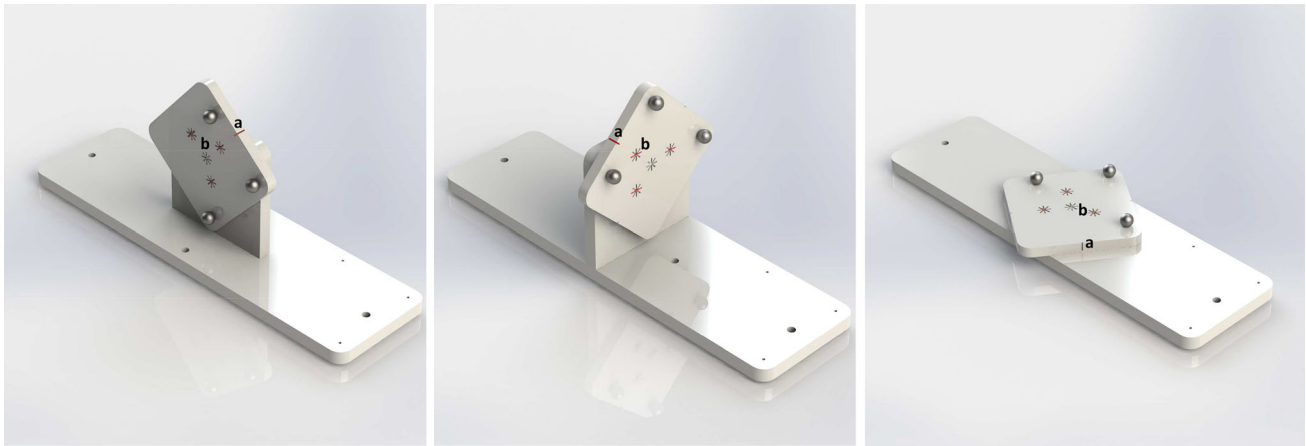


**Fig. 2** Design of the sensor construction for orientation measurements. In the photo from *left to right*, the setup for orientation around the  $x$ -,  $y$ -, and  $z$ -axis, respectively. The rod sensor could be mounted in-line with the rotation axis ( $a$ ), or perpendicular to the rotation axis ( $b$ ). This

sensor plate could be positioned on the stackable boxes similar to the position sensor plate as shown in Fig. 1. The sensor plate is  $9 \times 9$  cm, and the optical sphere distances are 5.8, 7.2, and 9.0 cm apart

- system and represented by a  $4 \times 4$  homogeneous transform matrix  ${}^{EM}\mathbf{P}_{Sx}$ ;
- the pose of the sensor plate expressed in the optical coordinate system  ${}^{Opt}\mathbf{P}_{Sensorplate}$ ;
  - the pose of the optical reference sensor on the TTFG casing  ${}^{Opt}\mathbf{P}_{TTFG}$ .

To make the OTS data independent of the camera position, the pose of the sensor plate was calculated with respect to the pose of the reference sensor using:

$$\begin{aligned} {}_{OTS}^{TTFG}\mathbf{P}_{Sensorplate} &= {}^{TTFG}\mathbf{P}_{Opt} {}^{Opt}\mathbf{P}_{Sensorplate} \\ &= {}^{Opt}\mathbf{P}_{TTFG}^{-1} {}^{Opt}\mathbf{P}_{Sensorplate} \end{aligned} \quad (1)$$

The additional subscript “OTS” explicates the fact that the measurement is accomplished with the OTS. Thus,  ${}_{OTS}^{TTFG}\mathbf{P}_{Sensorplate}$  reads as “the pose of the sensor plate, expressed in TTFG coordinates, but obtained from OTS data”. The registration between the coordinate systems was described by transformation matrix  ${}^{EM}\mathbf{M}_{TTFG}$ , bringing the optical coordinate system to the EM coordinate system. With Eq. 2, the pose of the optical tracker of the sensor plate transformed to the EM coordinate system

$${}_{OTS}^{EM}\mathbf{P}_{Sensorplate} = {}^{EM}\mathbf{M}_{TTFG} {}_{OTS}^{TTFG}\mathbf{P}_{Sensorplate} \quad (2)$$

For each EM sensor  $Sx$ ,  $x = 1, \dots, 4$ , a transformation matrix  ${}^{Sensorplate}\mathbf{M}_{Sx}$  was calculated from the OTS data, to express the sensor pose in EM coordinates:

$${}_{OTS}^{EM}\mathbf{P}_{Sx} = {}_{OTS}^{EM}\mathbf{P}_{Sensorplate} {}^{Sensorplate}\mathbf{M}_{Sx} \quad (3)$$

This pose was used as the reference.

For calibration, first, a dataset was acquired to estimate  ${}^{EM}\mathbf{M}_{TTFG}$ . The sensor plate was positioned and measured in the center of the TTFG at 12 cm distance. Subsequently, the sensor plate was positioned approximately plus and minus 10 cm along the  $x$ -axis and the  $y$ -axis, resulting in five measured positions per sensor. This was repeated at a distance of 22 cm above the TTFG. At each position, 10 measurements were acquired and subsequently averaged. For each EM sensor, we calculated the 3D vector between the 10 measured positions, resulting in 45 distance vectors in the EMTS coordinate system. Subsequently, a simplex optimization procedure was used to optimize  ${}^{EM}\mathbf{M}_{TTFG}$  to bring the OTS coordinate system to the EMTS coordinate system.

Secondly, a dataset was acquired to estimate  ${}^{Sensorplate}\mathbf{M}_{Sx}$  for each sensor. For this, the sensor plate was positioned four times in the center of the TTFG at a height of 12 cm, each time rotating the plate  $90^\circ$  around the  $z$ -axis of the EMTS. At each pose, 10 measurements were acquired and subsequently averaged. For each pose  ${}_{OTS}^{TTFG}\mathbf{P}_{Sensorplate}$  was transformed to EM coordinates  ${}_{OTS}^{EM}\mathbf{P}_{Sensorplate}$  using Eq. 2. Subsequently, the transform from  ${}_{OTS}^{EM}\mathbf{P}_{Sensorplate}$  to each measured EM sensor pose, i.e.  ${}_{EMTS}^{EM}\mathbf{P}_{Sx}$  was calculated, from which an estimate of  ${}^{Sensorplate}\mathbf{M}_{Sx}$  for each EM sensor was derived.

In a final step,  ${}^{EM}\mathbf{M}_{TTFG}$  and the four  ${}^{Sensorplate}\mathbf{M}_{Sx}$  matrices were further optimized using a simplex optimization method to minimize RMSE between  ${}_{OTS}^{EM}\mathbf{P}_{Sx}$  and  ${}_{EMTS}^{EM}\mathbf{P}_{Sx}$  using the whole calibration dataset. In this calibration procedure, only a small central area of the EM field close to the TTFG is used, resulting in a minimal RMSE in this area. This area was specifically chosen because the accuracy and jitter of EMTS are known to be proportional to the distance to the FG [13]. The resulting RMSE is provided as a measure of calibration accuracy.

## Measurements

All measurements were taken on a wooden table in a room with minimal EM field influence. Each of the below described measurements was repeated 5 times, including the above described calibration procedure, to make each measurement set independent.

### Positions

For the position accuracy measurements, the sensor plate with 4 sensors was positioned in 8 positions along the  $x$ -axis (5 cm spacing), repeated for 3 positions along the  $y$ -axis at 9 different distances along the  $z$ -axis from 12 to 52 cm above the TTFG. This resulted in a total of 864 measured sensor positions ( $5 \times 5 \times 5$  cm grid) [17], of which 716 were considered within the measurement volume according to the NDI Aurora system (Fig. 3). At each of the 716 measured positions, data were acquired for 10 s with a sample rate of 15 Hz, resulting in a total of 150 measurements per position, comparable to Maier-Hein et al. [13]. For each measured position, the jitter was defined as the standard deviation (SD) over the 150 measurements. For the accuracy estimation, we determined the RMSE, where for each position the average over the 150 measurements was compared with the average predicted sensor position as derived from Eq. 3. Jitter and RMSE were evaluated for the coordinates of the orthogonal axes separately, and also as vector.

Since the position accuracy was measured 5 times for each sensor set, the systematic and random components of local errors within the EM field could be evaluated. A thin-plate spline based non-rigid spatial mapping deformation vector field (DVF) was calculated between the estimated and measured sensor positions [18]. To correct for systematic spatial errors, the DVFs of the five measurements were averaged ( $\text{avgDVF}_{5\text{Dshielded}}$  and  $\text{avgDVF}_{6\text{Drod}}$ ). The average DVF was subsequently applied to each dataset to estimate the residual (random) errors.

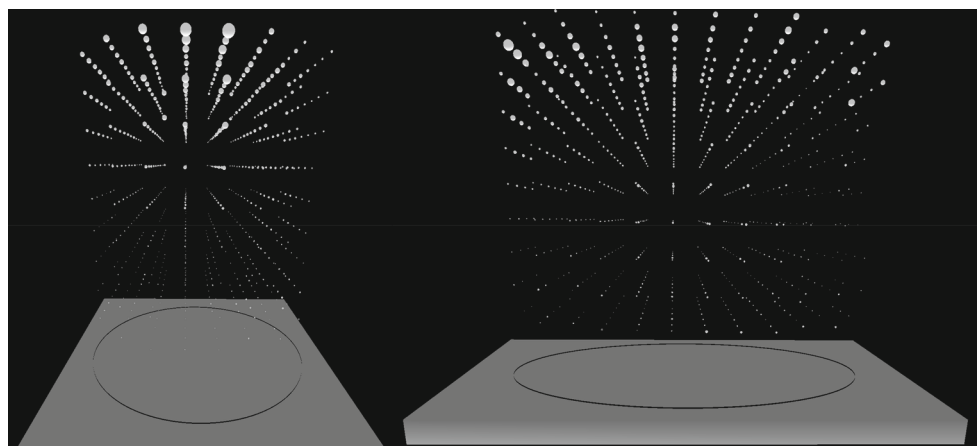
To evaluate if the local RMSE is sensor type dependent or general for the TTFG, an  $\text{avgDVF}_{\text{total}}$  was also calculated for the  $5\text{D}_{\text{shielded}}$  and  $6\text{D}_{\text{rod}}$  data together, and subsequently applied to the measurement sets to derive residual errors.

### Orientations

For the orientation accuracy, measurements were performed in the center of the TTFG, at heights along the  $z$ -axis of 17, 27, 37, and 47 cm. At each distance, orientation accuracy was measured with the rotation axis of the sensor plate along the  $x$ -,  $y$ -, and the  $z$ -axis of the EMTS separately. At each position and rotation axis, the sensor plate was rotated manually over  $360^\circ$  in 40 steps of approximately  $9^\circ$ . At each pose, 20 measurements were taken.

To derive the actual orientation of the rotation axis of the sensor plate in a single angle, the following procedure was used. Each sensor was positioned at a distance (at least 2 cm) to the actual rotation axis. Therefore the sensor positions describe a circle within their own coordinate system. For each sensor, a plane was fitted through the position data using least-squares fitting [19,20]. The plane was described as one 3D coordinate, and a vector perpendicular to the plane. The plane-vector was subsequently input for calculation of a quaternion vector rotation resulting in a quaternion describing the shortest arc rotation to a vector describing the  $y-z$  plane ( $V_{1,0,0}$ ). After transformation using the shortest arc quaternion, the resulting data described only orientations around the rotation axis. The data transformation was performed for both the OTS and EMTS data separately. To finally be able to compare both systems, the difference in rotation angle along the rotation axis of each measurement with respect to the previous measurement was calculated, resulting in 39 orientation angles per sensor per measurement set. The SD over the 20 measurements was calculated as the orientation jitter, and the average over the 20 measurements as orientation error.

**Fig. 3** Example RMSE visualized in 3D in the measurement field. In this example  $5\text{D}_{\text{shielded}}$  measurement 2 is shown. Each sphere is one measured position, the radius of the sphere depicts the actual vector error. For reference, the elliptical measurement field is outlined in black ( $60 \times 42$  cm) in the TTFG (gray)



For the  $6D_{rod}$  sensors, four sensors were used simultaneously, two positioned perpendicular to the rotation axis, and two positioned in line with the rotation axis. The  $6D_{disk}$  sensor could only be mounted on the surface of the sensor plate, perpendicular to the rotation axis. For the orientation measurements with three  $5D_{shielded}$  sensors, a least-squares fitting point match algorithm was used.

## Results

Acquisition of the position datasets took between 40 and 60 min per measurement set. In total 1.960.800 transform messages were stored. During acquisition of the first  $6D_{rod}$  measurement, the NDI aurora system indicated 3 times more invalid position measurements with increasing distance to the TTFG compared to other measurements. After about one-third of the data the position of the sensor cables with respect to the TTFG cable was altered, and invalid positions were no longer encountered.

### Position jitter

The average position jitter was very comparable between sensors and measurements, except for the first  $6D_{rod}$  measurement (Fig. 4), which was excluded from further jitter analysis. The average jitter in  $x$ -,  $y$ -, and  $z$ -direction was 0.027, 0.026 and 0.042 cm for  $5D_{shielded}$ , and 0.030, 0.032, and 0.049 cm for  $6D_{rod}$ , respectively. The jitter was exponentially proportional to the distance with the origin of the TTFG, and outliers up to 0.6 cm were present (Fig. 5). For comparison, with on average 0.003 cm jitter for both optical sensors, OTS jitter was much smaller.

### Calibration

The OTS and EMTS calibrations resulted in an average vector RMSE of 0.058 cm (range 0.048–0.062 cm) for the  $5D_{shielded}$

sensors, and 0.049 cm (range 0.044–0.052 cm) for the  $6D_{rod}$  sensors.

### Position accuracy

As shown in the spatial RMSE distribution in measurement 2 of the  $5D_{shielded}$  sensors (Fig. 3), the position accuracy is also varying with the distance to the TTFG (Fig. 6). In general, RMSE's were very comparable between the  $5D_{shielded}$  and  $6D_{rod}$  sensors. Despite the controlled environment, some measurements, such as  $5D_{shielded}$  measurement 1 and 4, and  $6D_{rod}$  measurement 2, seem to be less accurate than the other measurements (Fig. 6). In  $5D_{shielded}$  measurement 1 the reduced accuracy could be contributed to one single sensor, while in measurement 4 all sensors contributed to the reduced accuracy (not shown). In  $6D_{rod}$  measurement 2 the increased RMSE at 22 and 27 cm was due to all four sensors (not shown).

In Table 1 residual RMSE's are shown after correction of the measurements with the average DVF based on either all sensor specific measurements, or all measurements together. Both  $5D_{shielded}$  and  $6D_{rod}$  measurement 1 seem to be an outlier, with initial and residual RMSE  $\geq 0.16$  cm. The small differences between correcting with sensor specific data or the total dataset suggest that part of the position RMSE is system specific.

### Orientation jitter

There was very little orientation jitter for the optical sensor plate rigid body tool, on average  $0.006^\circ$  (range  $0.005^\circ$ – $0.009^\circ$ ). The 5 measurements per EM sensor type, position, and orientation were very reproducible, while the magnitude of orientation jitter between sensors was varying (Fig. 7). Combining three  $5D_{shielded}$  sensors to assess orientation resulted in orientation jitter of  $<0.1^\circ$  close to the TTFG, increasing to  $0.4$ – $0.9^\circ$  at 47 cm for the different orthogonal rotation axis. Orientation measurements were most stable

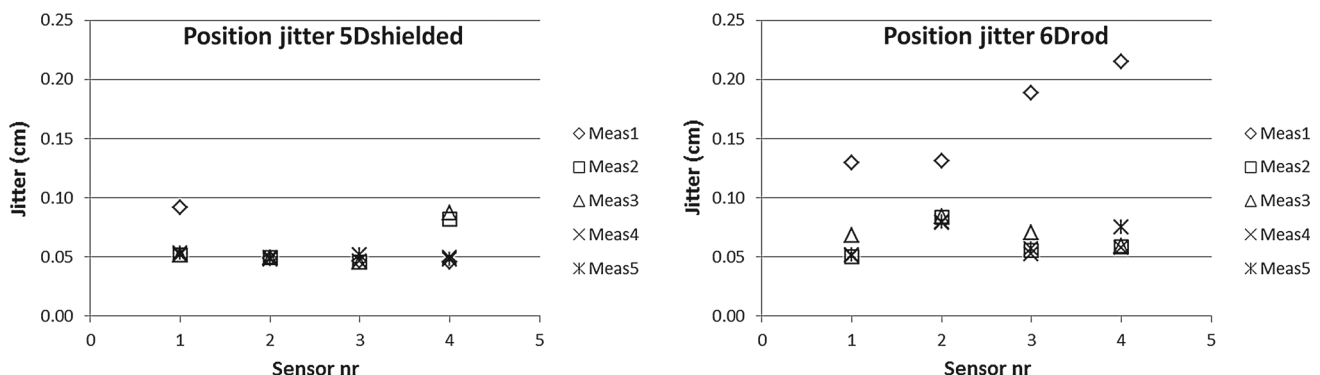
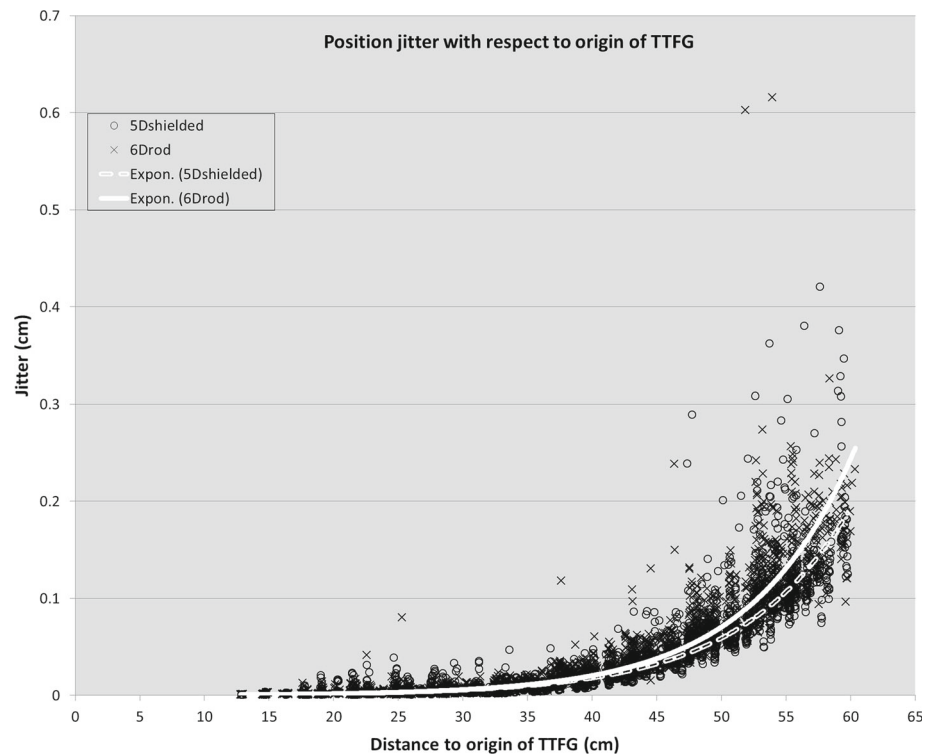


**Fig. 4** Vector jitter averaged over the entire measurement field for the different sensors and measurements

**Fig. 5** Vector jitter plotted for distance to the origin of the TTFG for both the 5D<sub>shielded</sub> and 6D<sub>rod</sub> data. An exponential trend line is added for both sensor sets, both fitting with an  $r^2$  of 0.9



with the 6D<sub>disk</sub> (all within 0.11° jitter). With the 6D<sub>rod</sub> oriented perpendicular to the rotation axis, orientation jitter was within 0.20°, while positioning the sensor in-line with the rotation axis resulted in jitter of 2.5–4.5° at 47 cm when rotated along the z-axis.

### Orientation accuracy

Similar to the jitter, the orientation accuracy was also varying for the different EM sensors (Fig. 8). The 6D<sub>disk</sub> was most accurate, with RMSE values ranging from 0.02 to 0.34°. For the 6D<sub>rod</sub> positioned perpendicular to the rotation axis, RMSE values were slightly larger, mainly at a distance of 47 cm above the TTFG (max 0.49°). With the 6D<sub>rod</sub> in-line with the rotation axis and the combined 5D<sub>shielded</sub> sensors, the RMSE was within 1.2° up to a distance of 37 from the TTFG. At a larger distance to the TTFG, both sensors become substantially less accurate.

### Discussion

In this study we compared the position and orientation accuracy of standard electromagnetic 5DOF and 6DOF sensors. The position accuracy was shown to be dependent on the distance between the sensor and the field generator and was very comparable between the sensor types. For the orientation accuracy, the results ranged from sub-degree (<0.4°

RMSE) for the 6D<sub>disk</sub>, to errors of several degrees at larger distance to the field generator for the combined 5D<sub>shielded</sub> sensors and the 6D<sub>rod</sub> sensor in-line with the rotation axis.

For rectal tumor tracking, we would like to address both position and orientation information. Our surgeons would like to have a 1 mm and 1° accuracy. To achieve this, three possible scenarios are available with the current system. Scenario 1: one single 6D<sub>rod</sub> sensor is implanted, providing information on position and orientation of the tumor. Scenario 2: two 5DOF sensors are implanted and combined to provide 6DOF information (similar to the 6D<sub>disk</sub>). Scenario 3: three (or more) 5D<sub>shielded</sub> sensors are implanted in the periphery of the tumor, and their position data are used to derive position and orientation. Wagner et al. have already shown in a porcine study that implantation of a wired sensor in the esophagus was feasible [12]. Still, because of the wired nature of the sensors, implantation of less sensors is preferred. Simultaneously, tracking accuracy is also dependent on the fixation of implanted sensors. Sensor migration in scenario 1 will have a larger impact on the TRE of the tumor compared to scenario 3, where the use of multiple sensors will reduce the impact of sensor migration. Similarly, tumor deformation can also result in target registration errors. For the remainder of the discussion, we assume to have perfectly fixed implanted sensors in a rigid tumor.

In terms of positions, there were no measurable differences between the 5D<sub>shielded</sub> sensor and the 6D<sub>rod</sub> sensor. Both position jitter and accuracy were comparable, and

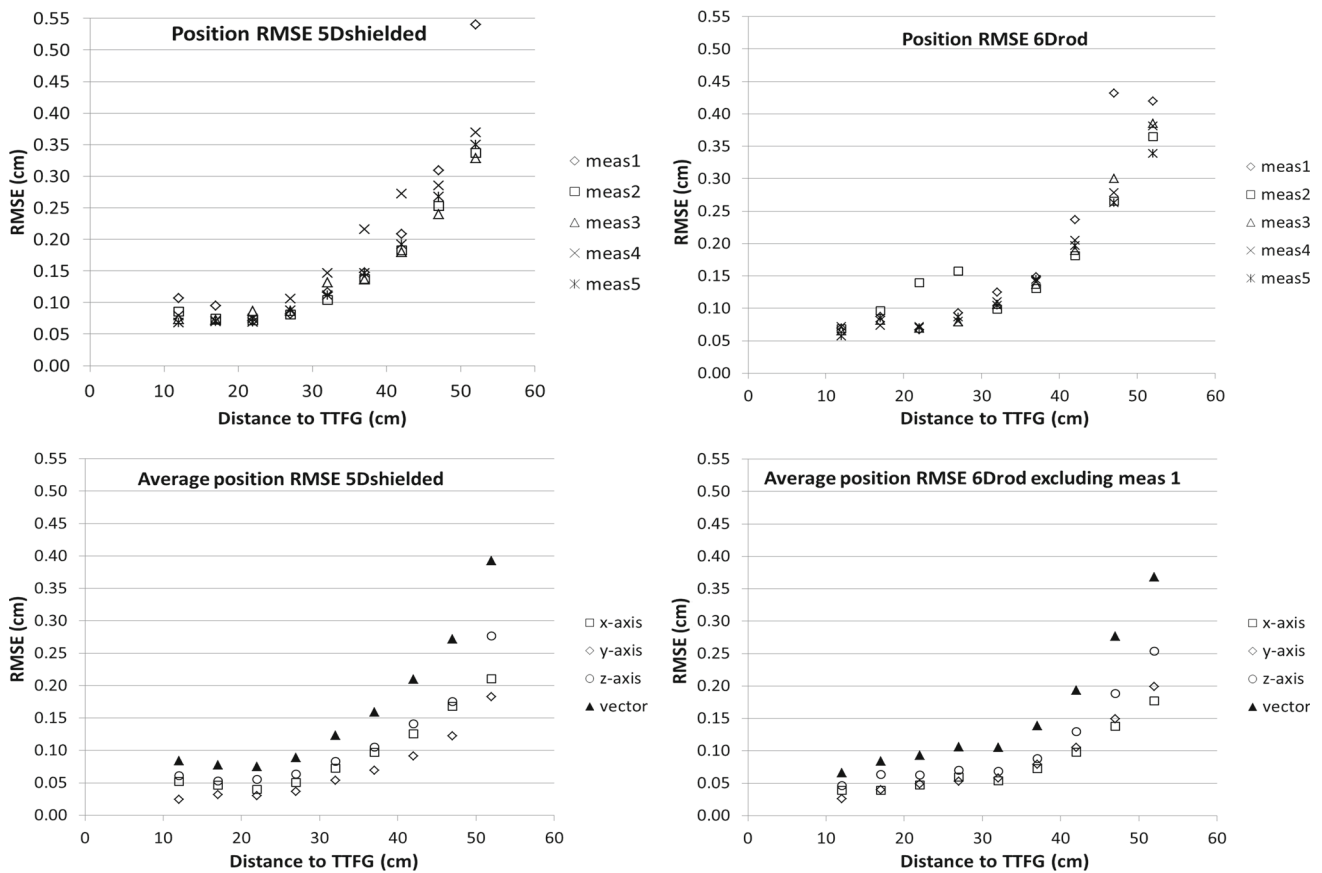


**Fig. 6** Position RMSE with respect to the distance to the TTFG for both sensor sets. In the *top row* the vector RMSE for the 5 measurements with the 5D<sub>shielded</sub> sensors (*left*) and 6D<sub>rod</sub> sensors (*right*). *Bottom row* the average RMSE separated for the orthogonal axes for 5D<sub>shielded</sub> (*left*) and 6D<sub>rod</sub> (*right*). Measurement 1 of the 6D<sub>rod</sub> sensors was excluded from the average due to cabling problems

**Table 1** Reproducibility of RMSE over the different measurements

In cm	RMSE no correction	RMSE after correction using $\text{avgDVF}_{5D_{\text{shielded}}}$	RMSE after correction using $\text{avgDVF}_{\text{total}}$
<b>5D<sub>shielded</sub></b>			
Meas. 1	0.24	0.16	0.18
Meas. 2	0.17	0.07	0.08
Meas. 3	0.17	0.07	0.09
Meas. 4	0.21	0.10	0.12
Meas. 5	0.18	0.06	0.07
In cm	RMSE no correction	RMSE after correction using $\text{avgDVF}_{6D_{\text{rod}}}$	RMSE after correction using $\text{avgDVF}_{\text{total}}$
<b>6D<sub>rod</sub></b>			
Meas. 1	0.23	0.18	0.21
Meas. 2	0.19	0.07	0.09
Meas. 3	0.19	0.07	0.08
Meas. 4	0.19	0.07	0.08
Meas. 5	0.18	0.07	0.10

Here the average local errors of either the sensor specific datasets were used to correct for the measurements or the average local errors of all datasets



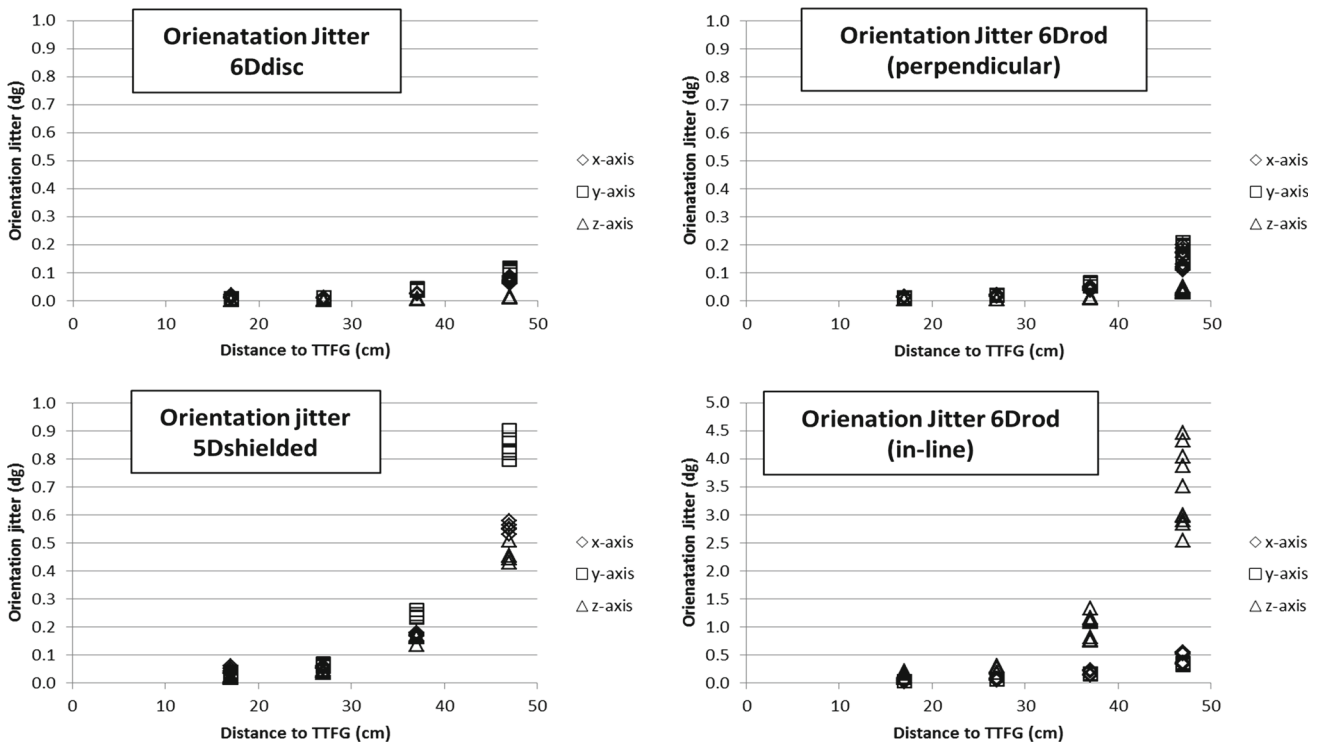


**Fig. 7** Orientation jitter for the different evaluated sensors. Note that the vertical axis of 6Drod in-line measurements (*lower right*) is scaled differently from the other figures

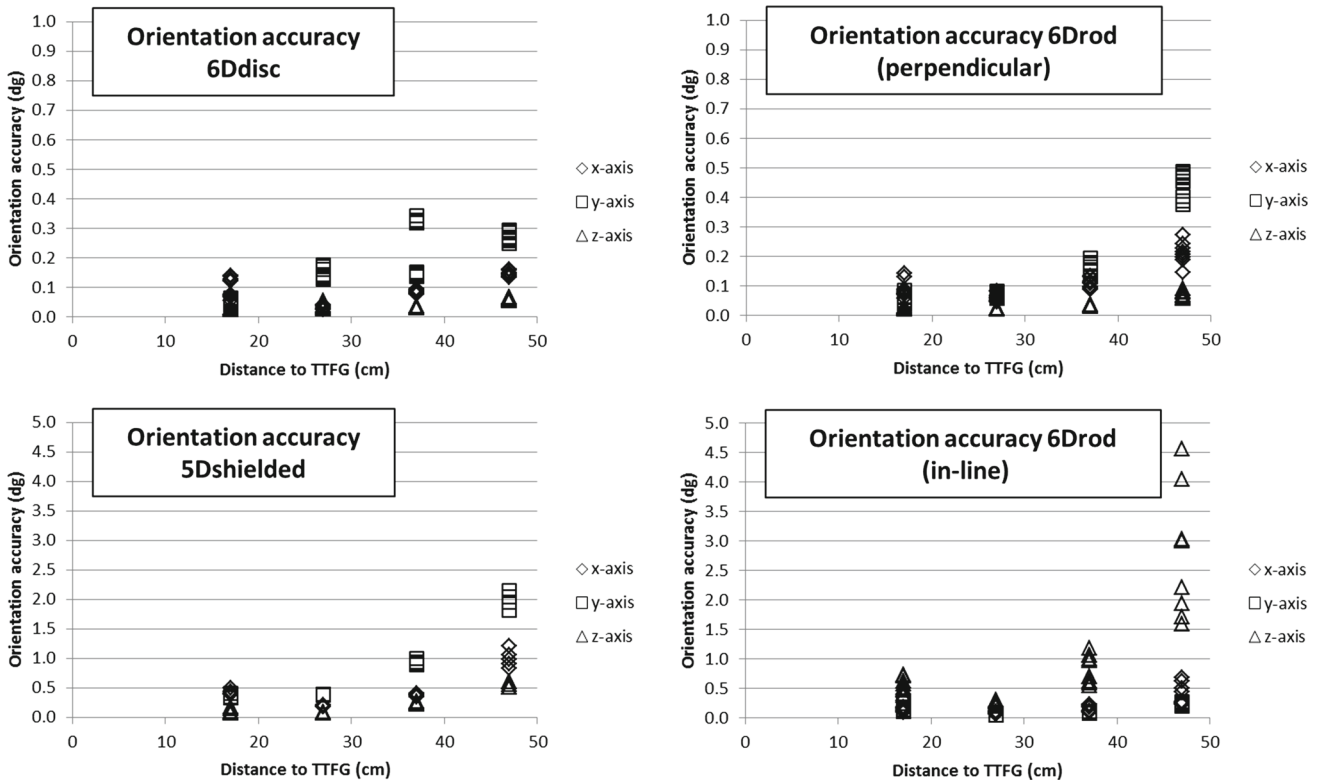


**Fig. 8** Orientation accuracy for the different evaluated sensors. Note that the scale of the vertical axis of *bottom* images is different from the images on the *top*

dependent on the distance to the TTFG (Fig. 5, 6, 7, 8). Jitter results were comparable to literature (0.02 mm at 15 cm to 0.09 mm at 35 cm [13]). The shown exponential relation (Fig. 5) suggests that position jitter can pose a substantial problem at larger distance to the TTFG. The position accuracy was comparable between both sensor sets and was approximately 0.1 cm RMSE up to 32 cm from the TTFG. At larger distances, the errors increased substantially, up to 0.4 cm RMSE at 52 cm from the TTFG. Similar results were also established with the standard bedside NDI Aurora field generator, at limited distance [14]. These results suggest that tumor tracking in terms of positions should be done within approximately 30 cm from the TTFG to assure an accuracy of approximately 0.1 cm RMSE and that it is independent of the sensor type.

For the incorporation of orientations in tumor tracking, differences were shown between the possible sensor implantation scenario's. For one 6D<sub>rod</sub>, orientation jitter and accuracy was established within 1° for all positions and orientations, except when the rotation was around the *z*-axis with the sensor in line with the rotation axis (Fig. 8). In the latter situation the rotation jitter and error increased beyond 1° at a distance of 37 cm from the TTFG. As expected from the position accuracy, orientation accuracy in scenario 3 was acceptable at close range, but decreased substantially at large distance from the TTFG (e.g. 47 cm). The best orientation accuracy was achieved with 6D<sub>disk</sub>, but was only slightly better than 6D<sub>rod</sub>. These data imply that in the measurement volume to approximately 30 cm from the TTFG all scenario's result in acceptable orientation accuracy with 1° RMSE. Orientation results were comparable to the data provided by Maier-Hein et al., who reported an average relative rotation error of 0.7° (in 15–35 cm from the TTFG) [13]. The use of position information of three EM sensors to derive orientation data has also been described by Franz et al., using the wireless Calypso system. In their discussion they indicated orientation errors of 0.12°, using sensor distances which are very comparable to our setup. Their results were more accurate than our setup, which is mainly due to more accurate position data using the Calypso system. We were not able to identify relevant literature comparing the use of different sensors or the separate orthogonal axes for orientation measurements.

The jitter and accuracy for both positions and orientations were shown to be dependent on the distance to the field generator (Figs. 5, 6, 7, 8). Therefore, caution is needed in comparing results to other published data. There is no single number representing the accuracy or jitter of a tracking system. The most comparable study evaluating the TTFG is by Maier-Hein et al. [13]. They evaluated jitter and accuracy of a 5DOF sensor at 15, 25 and 35 cm distance to the TTFG for 56 (8 rows by 7 columns, 5 cm distance) positions in plane. It is important to note that this is still not the entire

work field, since it is possible to measure 12 × 8 positions in plane (Fig. 3). We actually noticed that measurements at the edge of the oval *xy*-plane were sometimes less reliable. Furthermore, in 6D<sub>rod</sub> position measurement 1 there was a clear outlier in terms of jitter (Fig. 5), which was due to the position of the sensor cables. The five repeated position accuracy measurements per sensor type also indicated varying accuracy (Fig. 6), sometimes due to one sensor, sometimes all four. Similar effects were also described in literature [13] and demand for caution in the setup of measurements, even in a controlled environment.

Our measurement setup was inspired on the work of Hummel et al. and Maier-Hein et al. [13, 21]. Their setup is mainly focused on relative distances, but 3D errors throughout the volume are also assessed using accumulation of distances [13] or grid matching [21]. We chose to use an OTS as reference for assessment of absolute 3D errors throughout the measurement volume. The stackable boxes and use of multiple sensors provide flexibility and speed in sampling of the measurement volume, while the use of an OTS as reference makes reproducibility of sensor positioning less strict. The disadvantage of using an OTS as reference is the need for a calibration procedure to link the coordinate systems of both tracking systems. In our study, the residual position RMSE after calibration was 0.06 and 0.05 cm for 5D<sub>shielded</sub> and 6D<sub>rod</sub>, respectively. The calibration results indicate the lower limit of EMTS accuracy measurable with this system setup. As the stackable boxes are not as rigid as the Hummel setup, direct comparison of our measurements with literature [13, 21] is not available.

In our setup ideal measurement conditions were used. In clinical practice, the environment in which the procedure is done will influence the accuracy of the EMTS system [15, 22]. For example, in the intervention radiology setting near a CT scanner accuracy of the TTFG can decrease by a factor 3 [13]. We have shown that part of the position inaccuracies were systematic (Table 1) and can be corrected. The average DVF of the sensor specific data and the total dataset both could be used to substantially decrease the RMSE. Hummel et al. also described improved accuracy after calibration of the field generator by the manufacturer [21], indicating that there is a systematic component to the position RMSE. During surgery, safety measures should be in place to monitor the actual accuracy of the tracking system. The actual accuracy of a clinical application which makes use of EMTS is dependent on the total error model of the system. For every new application, the error model should be composed, and results from the current study might be beneficial to estimate parts of the total model.

It is important to note the influence of the cable wiring, as was shown in position measurement 1 of the 6D<sub>rod</sub> sensor. We adapted the cable positions with respect to each other, the TTFG and the TTFG cable until the bad measurements, indi-

cated by the NDI software, were gone. An actual systematic approach with guidelines would be convenient in the future.

We only evaluated the static position and orientation accuracy, while dynamic measurements might be less reliable. Furthermore, we only evaluated the orientation accuracy using the positions of multiple 5D<sub>shielded</sub> sensors in one fixed configuration. The orientation accuracy in this setup is dependent on the sensor distance, and thus also tumor size. The position accuracy data of this study can, however, be used to estimate the orientation accuracy with other sensor distances. In this study, an OTS was used as reference standard and was assumed to be perfect. Although OTS is known to be much more accurate than EMTS, remaining errors are present, and are masked in the presented EMTS results. The optical markers of the OTS system were mounted on standard stainless steel sphere mounts, which subsequently might influence the magnetic field of the EMTS system. The actual type of stainless steel is unknown to us, but it will probably be an austenitic type, as many surgical tools are, which has minor influence on the magnetic field. We made sure that the sphere mounts were at least at a 3 cm distance from the EM sensors.

In this study we focused on the setting of tumor tracking. Other topics of interest which can also be interesting are tracking of steerable camera's such as bronchoscopes, or coloscopes. In particular, the interaction of accuracy with other equipment and the dynamic behavior can be interesting.

## Conclusions

We have compared the position and orientation accuracy of standard electromagnetic 5DOF and 6DOF sensors. The position accuracy was shown to be dependent on the distance between the sensor and the field generator, and was very comparable between the sensor types. For the orientation accuracy, the results ranged from sub-degree errors close to the field generator, to errors of several degrees at larger distances. The orientation accuracy was sub-degree when using the 6D<sub>disk</sub> sensor and was also within 0.5° when using the 6D<sub>rod</sub> sensor, except for one orientation of the 6D<sub>rod</sub> sensor. Combining the position data of 3 sensors in a volume of 4 cm diameter resulted in larger orientation errors of one to several degrees. For practical applications, such as tracking of rectal tumors during surgery using an electromagnetic system, it is important to minimize the distance to field generator. Independent of the sensor type, tracking accuracy within 30 cm of the field generator can be expected in the order of 1 mm and 1°.

**Acknowledgments** We would like to thank Sander Biersteker and Ton Vlasveld of the Netherlands Cancer Institute for their help in the design and construction of the measurement setup. This research was supported by Maurits en Anna de Kock Stichting, Breuning ten Cate

Fonds, and KWF-Alpe d'HuZes (NKI 2014-6596). We are very grateful for their support.

## Compliance with ethical standards

**Conflict of interest** There is no conflict of interest to report for this article.

## References

1. Grunert P, Darabi K, Espinosa J, Filippi R (2003) Computer-aided navigation in neurosurgery. *Neurosurg Rev* 26:73–99 discussion 100–1
2. Senft C, Ulrich CT, Seifert V, Gasser T (2010) Intraoperative magnetic resonance imaging in the surgical treatment of cerebral metastases. *J Surg Oncol* 101:436–41. doi:10.1002/jso.21508
3. Langø T, Tangen GA, Mårvik R, Ystgaard B, Yavuz Y, Kaspersen JH, Solberg OV, Hernes TAN (2008) Navigation in laparoscopy-prototype research platform for improved image-guided surgery. *Minim Invasive Ther Allied Technol* 17:17–33. doi:10.1080/13645700701797879
4. Aschendorff A, Maier W, Jaekel K, Wesarg T, Arndt S, Laszger R, Voss P, Metzger M, Schulze D (2009) Radiologically assisted navigation in cochlear implantation for X-linked deafness malformation. *Cochlear Implants Int* 10(Suppl 1):14–18. doi:10.1002/cii.379
5. Wong K-C, Kumta S-M (2014) Use of computer navigation in orthopedic oncology. *Curr Surg Rep* 2:47. doi:10.1007/s40137-014-0047-0
6. Sugimoto M, Yasuda H, Koda K, Suzuki M, Yamazaki M, Tezuka T, Kosugi C, Higuchi R, Watayo Y, Yagawa Y, Uemura S, Tsuchiya H, Azuma T (2010) Image overlay navigation by markerless surface registration in gastrointestinal, hepatobiliary and pancreatic surgery. *J Hepatobiliary Pancreat Sci* 17:629–636. doi:10.1007/s00534-009-0199-y
7. Soler L, Nicolau S, Pessaux P, Mutter D, Marescaux J (2014) Real-time 3D image reconstruction guidance in liver resection surgery. *Hepatobiliary Surg Nutr* 3:73–81. doi:10.3978/j.issn.2304-3881.2014.02.03
8. Elfiring R, de la Fuente M, Radermacher K (2010) Assessment of optical localizer accuracy for computer aided surgery systems. *Comput Aided Surg* 15:1–12. doi:10.3109/10929081003647239
9. Zhang H, Banovac F, Lin R, Glossop N, Wood BJ, Lindisch D, Levy E, Cleary K (2006) Electromagnetic tracking for abdominal interventions in computer aided surgery. *Comput Aided Surg* 11:127–136. doi:10.1002/igs.10025
10. Gosens MJEM, Klaassen RA, Tan-Go I, Rutten HJT, Martijn H, van den Brule AJC, Nieuwenhuijzen GAP, van Krieken JHJM, Nagtegaal ID (2007) Circumferential margin involvement is the crucial prognostic factor after multimodality treatment in patients with locally advanced rectal carcinoma. *Clin Cancer Res* 13:6617–23. doi:10.1158/1078-0432.CCR-07-1197
11. Shihab OC, Brown G, Daniels IR, Heald RJ, Quirke P, Moran BJ (2010) Patients with low rectal cancer treated by abdominoperineal excision have worse tumors and higher involved margin rates compared with patients treated by anterior resection. *Dis Colon Rectum* 53:53–56. doi:10.1007/DCR.0b013e3181c70465
12. Wagner M, Gondan M, Zöllner C, Wünsch JJ, Nickel F, Alcala L, Groch A, Suwelack S, Speidel S, Maier-Hein L, Müller-Stich BP, Kenngott HG (2015) Electromagnetic organ tracking allows for real-time compensation of tissue shift in image-guided laparoscopic rectal surgery: results of a phantom study. *Surg Endosc*. doi:10.1007/s00464-015-4231-9
13. Maier-Hein L, Franz AM, Birkfellner W, Hummel J, Gergel I, Wegner I, Meinzer H-P (2012) Standardized assessment of new

- electromagnetic field generators in an interventional radiology setting. *Med Phys* 39:3424–34. doi:[10.1118/1.4712222](https://doi.org/10.1118/1.4712222)
14. Martens V, Kleemann M, Matthäus L, Bruch HP, Schweikard A (2006) Evaluation of EM tracking systems for laparoscopic liver surgery. *Int J CARS* 1:215–218
  15. Nafis C, Jensen V, von Jako R (2008) Method for evaluating compatibility of commercial Electromagnetic (EM) micro sensor tracking systems with surgical and imaging tables. 6918:691820-1–691820-15. doi:[10.1117/12.769513](https://doi.org/10.1117/12.769513)
  16. Lasso A, Heffter T, Rankin A, Pinter C, Ungi T, Fichtinger G (2014) PLUS: open-source toolkit for ultrasound-guided intervention systems. *IEEE Trans Biomed Eng* 61:2527–37. doi:[10.1109/TBME.2014.2322864](https://doi.org/10.1109/TBME.2014.2322864)
  17. Hummel JB, Bax MR, Figl ML, Kang Y, Maurer C, Birkfellner WW, Bergmann H, Shahidi R (2005) Design and application of an assessment protocol for electromagnetic tracking systems. *Med Phys* 32:2371–9
  18. Chui H, Rangarajan A (2003) A new point matching algorithm for non-rigid registration. *Comput Vis Image Underst* 89:114–141. doi:[10.1016/S1077-3142\(03\)00009-2](https://doi.org/10.1016/S1077-3142(03)00009-2)
  19. Hamilton WC (1961) On the least-squares plane through a set of points. *Acta Crystallogr* 14:185–189. doi:[10.1107/S0365110X61000620](https://doi.org/10.1107/S0365110X61000620)
  20. Schomaker V, Waser J, Marsh RE, Bergman G (1959) To fit a plane or a line to a set of points by least squares. *Acta Crystallogr* 12:600–604. doi:[10.1107/S0365110X59001748](https://doi.org/10.1107/S0365110X59001748)
  21. Hummel J, Figl M, Birkfellner W, Bax MR, Shahidi R, Maurer CR, Bergmann H (2006) Evaluation of a new electromagnetic tracking system using a standardized assessment protocol. *Phys Med Biol* 51:N205–N210. doi:[10.1088/0031-9155/51/10/N01](https://doi.org/10.1088/0031-9155/51/10/N01)
  22. Franz AM, Haidegger T, Birkfellner W, Cleary K, Peters TM, Maier-Hein L (2014) Electromagnetic tracking in medicine—a review of technology, validation, and applications. *IEEE Trans Med Imaging* 33:1702–25. doi:[10.1109/TMI.2014.2321777](https://doi.org/10.1109/TMI.2014.2321777)